

**THE PROTEROZOIC ORÓS BELT, NORTHEAST BRAZIL:
GEOCHEMICALLY DIVERSE META-IGNEOUS ROCKS, LITHOLOGICAL ASSOCIATIONS
AND TECTONIC IMPLICATIONS**

I. McReath

ABSTRACT

The meta-igneous rocks of the Proterozoic (c. 1.8 Ga) Orós belt occur near the base of a metamorphosed arenite-pelite-carbonate sequence. Locally, deeper water conditions are registered by the presence of turbidites. A short volcano-exhalative episode is recorded within the igneous-dominated horizons by a felsic tuff-chert-tourmalinite-oxide type BIF association. Compositions of the meta-igneous rocks vary widely over a present distance of about 200 km. Mafic magma types include T-MORB and CWPB. Sá et al. (1991) also reported the presence of a mafic-intermediate suite with geochemical characteristics suggesting that they are derived from a more enriched mantle. Felsic volcanics have geochemical characteristics of WPG to SCG. Taking into account the bimodal nature of most of the magmatism, together with the detritic sediment-dominated nature of the sequence as a whole, it is suggested that the Orós belt represents an intracontinental rift, which developed in relatively unattenuated crust and which may have evolved to a restricted ocean basin. Mafic magmas were produced by partial melting of undepleted to enriched mantle types, and mostly remained trapped at the base of the continental crust, where they caused extensive anatexis. This rift represented a major discontinuity in the post-Transamazonian continental crust, which probably influenced the behaviour of the crustal segments during the later Brasiliano (Pan-African) orogeny.

RESUMO

As rochas meta-ígneas do cinturão proterozóico (c. 1,8 Ga) de Orós ocorrem próximo à base de um conjunto metassedimentar continental, composto por arenitos, pelitos e rochas carbonatadas. Ocorreram, localmente, aprofundamentos d'água, registrados pela presença de turbiditos. Um episódio curto de natureza vulcano-exalativa manifesta-se, na parte da sequência dominada pelas rochas ígneas, pela associação tufos félsicos-"chert"-turmalinito-BIF do tipo óxido. As composições das rochas meta-ígneas apresentam importante variação ao longo de c. 200 km atuais do cinturão. As máficas incluem T-MORB e CWPB. Sá et al. (1991) notaram a presença de uma associação máfica-intermediária, cujas características geoquímicas acusam a participação de um manto enriquecido. As félsicas possuem assinaturas geoquímicas de WPG a SCG. Levando-se em conta a natureza bimodal da maior parte dos produtos magmáticos, bem como a dominância das rochas metassedimentares, conclui-se que o cinturão de Orós representa um rift intracontinental, desenvolvido em crosta pouca atenuada que talvez evoluiu para uma bacia oceânica restrita. Magmas máficos formaram-se a partir de manto desde relativamente não empobrecido até enriquecido. A maior parte desses magmas ficou retido na base da crosta, causando anatexia. O rift representou uma descontinuidade importante na crosta pós-transamazônica. É provável que tal descontinuidade tenha influenciado o comportamento dos segmentos crustais, durante a orogenia brasileira (Pan-Africana) subsequente.

INTRODUCTION

The area studied lies within the Borborema Province of gneiss-migmatite terrains and fold belts of metamorphosed supracrustal rocks, situated north of the São Francisco Craton (Almeida et al., 1981, Fig. 1, inset (A)). While the craton largely escaped the tectono-magmatic effects of the late Proterozoic Brasiliano (Pan African) orogeny, the Borborema was intensely involved in this orogeny.

Prominent amongst the folded supracrustal sequences is the Orós belt, which forms a boomerang-shaped strip with a

total length of at least c. 425 km, and occurs in Ceará State (Fig. 1, inset (B)). The Jaguaribe belt is found nearby. Early, mostly regional scale studies of both belts were briefly summarized by Santos et al. (1984) and Santos & Brito Neves (1984). More recently, the N-S arm of the Orós belt (Fig. 1, main map (C)) has been the subject of more detailed studies (Braga & Mendonça, 1984; Mendonça & Braga (1987; Sá et al., 1988; Macedo et al., 1988; Sá, 1991), while the E-W arm counts with only isolated descriptions of detailed

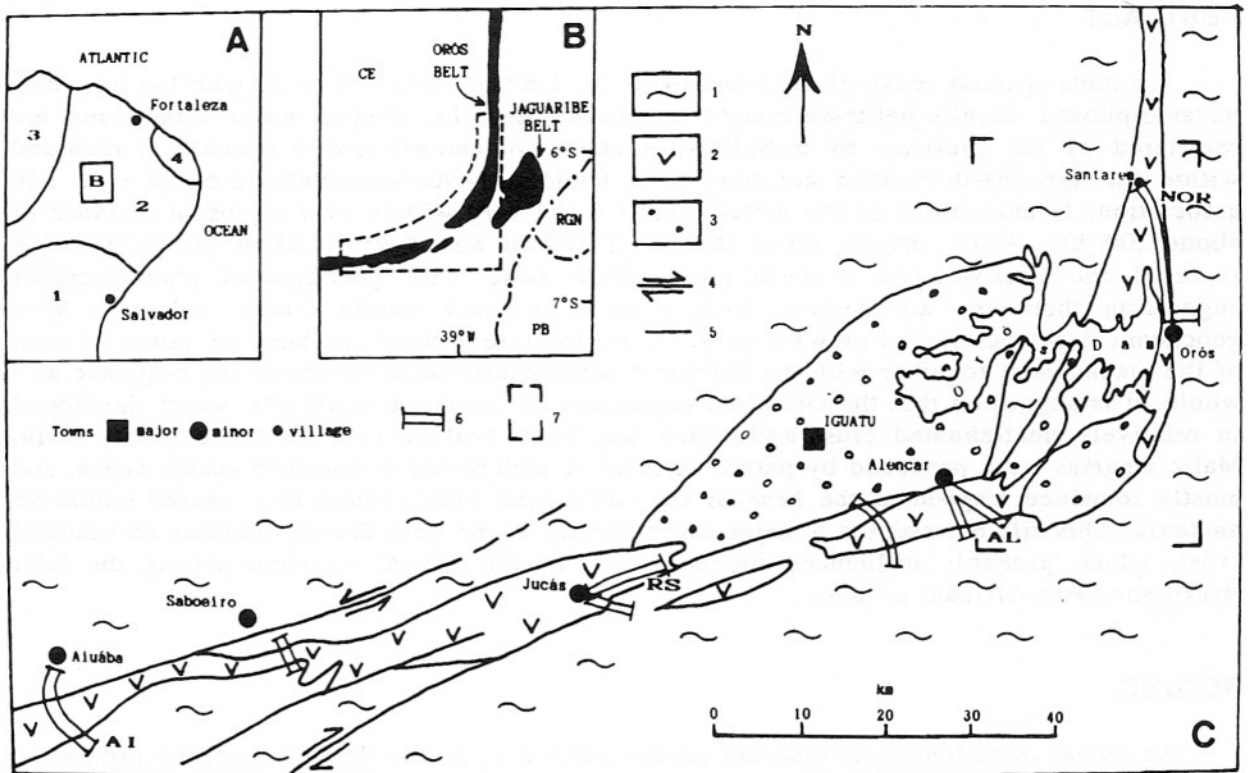


Figure 1 - Inset (A): tectonic elements of Northeast Brazil: 1- São Francisco Craton; 2- Borborema Province; 3- Paraíba and 4- Potiguar Phanerozoic basins. Inset (B): Main supracrustal sequences of southeastern Ceará. Outlined area, see main map (C). CE = Ceará; RGN = Rio Grande do Norte; PB = Paraíba. Main map (C): Geological ketch of study area, after DNPM (1983). 1- gneiss-migmatite basement; (2) Orós metavolcano-sedimentary sequences; (3) Phanerozoic sediments; 4- shear zones and sense of movement; 5- contacts; 6- geological sections; 7- area studied by Sá et al. (1988, 1991); Sá (1991).

profiles (Ries, 1977; Bodenlos, 1950 in: Santos et al., 1984). In fact, there is considerable divergence as to the surface expression of the supracrustal sequence in the sector in small-scale studies (e.g. DNPM, 1974, 1983).

This article presents the results of a reconnaissance petrographical and geochemical study of meta-igneous rocks from the Orós belt, mostly from its E-W arm. Taking into account the geochemical affinities of these rocks and the lithological associations found, the possible early geological evolution of the belt is discussed.

GEOLOGICAL OUTLINE OF THE ORÓS BELT

The N-S arm

The sequence is dominated by an arenite-pelite-carbonate, shallow-water assemblage, locally with turbidites representing

deeper water facies. The igneous component includes volcanic rocks deposited near the base of the supra-crustal sequence. Sá (1991) and Sá et al. (1991) compared the basal mafic-intermediate association to volcanic arc shoshonites on the basis of similarities between multi-element spectra ("spidergrams"). Felsic volcanics stratigraphically above rocks of the mafic-intermediate suite have a different ($^{87}\text{Sr}/^{86}\text{Sr}$) initial ratio ($R_i = 0.702$) from that of the andesites of the suite ($R_i = 0.705$; Macedo et al., 1988; Sá, 1991), and have "spidergrams" which are typical of within-plate granites (WPG). These felsic rocks are therefore not cogenetic with the mafic-intermediate suite. The age of the felsic volcanics, together with associated intrusive rocks, shows that the deposition of the sequence commenced between 1.8 and 1.7 Ga (Macedo et al., 1988; Sá et al., 1991).

Samples from two profiles in the N-S arm were studied during this investigation.

Table 1 – Analyses of meta-igneous rocks from the Orós belt - major and minor elements (wt%) and trace elements (ppm).

	(1)	(2)	A11	A12	A13	RS1	RS2	RS3	AL1
SiO ₂	1.0	2.0	48.8	61.1	72.4	68.1	68.7	70.8	43.5
TiO ₂	2.0	5.0	2.6	0.92	0.18	0.44	0.35	0.36	1.8
Al ₂ O ₃	1.0	5.0	13.0	16.1	13.2	15.1	15.2	13.7	9.1
Fe ₂ O ₃	1.0	2.0	8.4	2.0	0.60	1.2	1.4	1.3	2.8
FeO	5.0	10.0	5.81	5.10	0.99	2.12	1.84	1.34	10.49
MnO	5.0	5.0	0.25	0.13	0.02	0.05	0.05	0.03	0.22
MgO	2.0	2.0	4.2	2.6	0.36	1.2	1.3	0.67	17.2
CaO	1.0	1.0	12.1	3.7	1.3	2.3	3.1	1.2	8.2
Na ₂ O	1.0	5.0	2.5	3.2	3.4	4.6	4.9	3.3	0.36
K ₂ O	1.0	1.0	0.31	3.5	6.8	3.6	1.9	5.9	0.08
T.V. ⁽³⁾			1.68	1.29	0.46	1.11	0.89	1.15	5.94
P ₂ O ₅	5.0	5.0	0.32	0.35	0.16	0.20	0.12	0.15	0.34
Total			99.97	99.99	99.87	99.02	99.51	99.90	99.03
Rb	10	20	<10	190	140	77	230	45	<10
Sr	5	10	190	250	310	740	640	250	73
Ba	5	10	85	700	1730	1120	1090	1280	67
Ni	5	10	84	-	-	-	-	-	600
Cr	10	20	152	-	-	-	-	-	1048
Y	10	30	68	72	<10	40	20	17	56
Zr	10	20	130	220	150	270	190	330	92
La	10	20	28.5	33.0	31.0	37.6	11.0	74.2	-
Ce	10	10	63.2	78.2	69.3	83.8	21.0	158.2	-
Nd	10	10	30.5	31.2	23.6	29.0	12.3	42.3	-
Sm	10	10	8.5	8.3	4.9	5.6	3.2	7.8	-
Eu	10	10	1.9	1.2	0.52	0.97	0.47	1.1	-
Gd	10	10	6.3	5.7	2.3	2.5	1.6	3.4	-
Dy	10	10	6.0	4.6	1.3	1.6	1.4	1.8	-
Ho	20	50	1.2	0.82	0.20	0.22	0.22	0.23	-
Er	10	20	3.5	2.4	0.50	0.60	0.61	0.65	-
Tm	20	50	0.52	0.39	0.08	0.10	0.10	0.11	-
Yb	10	20	3.7	2.6	0.75	0.79	0.74	0.82	-
Lu	20	50	0.39	0.32	0.14	0.10	0.09	0.09	-

(Continuation Table 1)

	AL2	AL3	AL4	AL5	AL6	AL7	NOR1	NOR2	NOR3
SiO ₂	44.7	47.0	48.0	48.1	48.0	66.7	47.0	48.9	74.9
TiO ₂	1.0	1.8	1.2	1.2	0.88	0.77	2.5	3.6	0.68
Al ₂ O ₃	12.6	11.9	14.7	13.6	13.0	14.2	12.8	12.6	11.9
Fe ₂ O ₃	5.0	3.3	1.7	2.8	2.3	1.2	5.4	8.6	1.6
FeO	6.09	1.06	10.35	9.64	8.15	4.39	4.25	6.38	1.84
MnO	0.19	0.21	0.20	0.19	0.19	0.07	0.16	0.22	0.05
MgO	17.2	10.5	6.9	8.3	8.9	3.0	6.2	5.2	0.68
CaO	18.9	9.1	13.3	12.1	13.3	1.8	14.4	9.5	0.99
Na ₂ O	0.71	1.9	1.8	1.9	2.1	3.5	3.0	3.0	2.7
K ₂ O	0.12	0.15	0.17	0.13	0.22	2.6	0.29	0.17	3.0
T.V. ⁽³⁾	3.94	3.72	1.8	2.01	2.00	1.60	3.52	1.51	1.00
P ₂ O ₅	0.12	0.40	0.12	0.11	0.09	0.26	0.43	0.43	0.16
Total	100.27	100.04	100.24	100.08	100.13	99.49	100.45	100.11	99.50
Rb	<10	<10	<10	<10	<10	77	<10	<10	130
Sr	380	1280	200	160	140	140	700	260	140
Ba	24	78	14	54	43	660	170	55	530
Ni	156	440	140	140	160	-	150	50	-
Cr	248	819	438	114	362	-	-	-	-
Y	36	64	44	34	28	34	26	67	16
Zr	77	340	83	79	44	120	230	220	220
La	-	-	-	-	2.4	-	47.9	28.5	34.8
Ce	-	-	-	-	12	-	94.7	71.0	80.4
Nd	-	-	-	-	6.2	-	37.0	34.4	28.5
Sm	-	-	-	-	1.9	-	8.5	10.0	7.5
Eu	-	-	-	-	0.62	-	2.2	2.3	1.0
Gd	-	-	-	-	1.9	-	5.6	7.0	4.8
Dy	-	-	-	-	2.3	-	3.7	5.6	4.1
Ho	-	-	-	-	0.48	-	0.61	1.1	0.80
Er	-	-	-	-	1.4	-	1.7	3.1	2.4
Tm	-	-	-	-	-	-	0.24	0.43	0.42
Yb	-	-	-	-	1.1	-	1.3	2.7	2.7
Lu	-	-	-	-	0.12	-	0.14	0.34	0.31

(1) Estimated relative probable precision 1σ (%) based on data for replicate analyses and GEOLAB specifications

(2) Relative accuracy 1σ (%) based on comparison of literature recommended values and results obtained by GEOLAB

(3) Total volatiles = L.O.I. + 0.1113 x FeO (Lechlers & Desilets, 1987)

- not determined

Analysed samples reported here are from the NOR section, roughly along strike northwards from Orós (Fig. 1, main map (C)).

The E-W arm

Seven detailed profiles, together with intervening spot observations, were undertaken in the E-W arm. Analysed samples are from the AI, RS and AL profiles (Fig. 1, main map (C)). The observations generally confirm the map of DNPM (1983) as far as the supra-crustal rocks are concerned. The present outcrop pattern of the supracrustal rocks shows the strong influence of shearing whose last movement was dextral. Phanerozoic sediments cover a large part of the belt at the geometrical flexure point of the belt, between the towns of Alencar and Orós.

The sequence shows important differences from the pattern of the N-S arm only in the sector near Alencar. Santos et al. (1984, after Bodenlos, 1950) record the presence of abundant amphibolites. Some of these are associated with magnesite deposits, which could be the products of hydrothermal transformations of nearby marbles, or even of meta-ultramafic rocks which also occur there (Braga & Mendonça, 1984). On the other hand, many of the amphibolites retain textural relicts which attest to their volcanics or plutonic origin.

In this sector, banded rocks composed of thin alternating felsic tuffs and predominantly cherty or tourmaliniferous beds are in close proximity both to a massive, fine-grained rock composed of c. 95% zoned tourmaline, and to oxide-type banded iron formation with local manganese enrichment. Together, these rocks probably represent a volcano-exhalative deposit of limited extent (<1 m thick x <3 km long).

Metamorphic history of the belt

The rocks are in low (sections AI and RS) to medium (sections AL and NOR) metamorphic grade. The latter rocks invariably show some signs of retrograde reactions. In some cases, these reactions were accompanied or followed by penetration of hydrothermal fluids along faults and fractures. A common mineral assemblage deposited by these fluids is represented by epidote \pm chlorite \pm carbonate minerals. As far as possible, in the analytical programme

samples with important quantities of this late assemblage were avoided.

Metamorphism accompanied polyphase deformation which largely destroyed primary igneous textures. Samples were selected on the basis of the presence of probably igneous relicts. On the other hand, a few rocks are simply schists, which were identified as probable metavolcanics on geological grounds. Brief descriptions are given in the Appendix.

GEOCHEMISTRY IN THE META-IGNEOUS ROCKS

Analytical methods

Major, trace and rare earth element analyses were undertaken by the commercial laboratory GEOLAB/GEOSOL, Belo Horizonte, Brazil, using the standard wet chemical and instrumental (AAS, XRF, etc.) methods adopted by this laboratory (e.g. rare earth elements by ion-exchange and ICP measurement: Dutra, 1984). During this and other projects, external quality control was performed by inclusion of hidden duplicates, local and international standards. Observed precision results and estimates of probable accuracy, using the most recent compilations of data for international standards available (e.g. Gladney & Roelandts, 1988; Gladney et al., 1990), are given in Table 1.

Screening of samples

Selection based on petrographical criteria reduced the original collection of over 50 candidate samples to about 40. Most of the samples rejected showed excessive hydrothermal or weathering modifications. Many of the remaining samples are schistose, and therefore chemical criteria, such as those proposed by Garrels & Mackenzie (1971) and La Roche (1972) for separating igneous and sedimentary rocks, were used to screen these samples.

At this point, light beige-coloured schists with quartz "eyes" and magnetite porphyroblasts, previously identified as possible felsic metavolcanics (AL9, NOR4) were rejected. They have intermediate SiO₂ contents (61-62%), high Al₂O₃ (19-21%), low Na₂O (0.53-0.65%), high K₂O (5.1-6.2%) and highly oxidized iron (Fe₂O₃/Fe₂O total = 0.78-0.83). Within the geological context, these rocks could be either

hydrothermally modified intermediate-felsic volcanic rocks, or products of intense tropical sub-aerial weathering derived from intermediate-acid volcanic protoliths.

Subsequently, the compositions of the remaining samples were compared to the igneous trends defined by Beswick & Soucie (1978) on log molecular proportion ratios (LMPR) plots. For mafic types, even samples which show petrographical and chemical evidence for advanced epidotization (high CaO contents, moderately to highly oxidized iron, low total alkalis contents: e.g. Condie et al., 1977; Jolly, 1980) do not depart far from the standard trends (examples given in Fig. 2) for a number of LMPR pairs. The mafic rocks have alteration indexes (A.I. = $(\text{MgO} + \text{K}_2\text{O}) / (\text{MgO} + \text{K}_2\text{O} + \text{Na}_2\text{O} + \text{CaO}) \times 100$: Hacheguchi (1983) in Laflèche et al. (1992)), in the range 23.6 (sample No. AI1) to 40.8 (AL5). A.I. values for AL4, AL5, AL6 and NOR2 are within the range 36 ± 8 , considered normal for non-cumulate mafic rocks. In contrast, some felsic rocks do not conform to the Beswick & Soucie (1978) igneous trends, but all analyses fall within Hughes' (1973) "igneous spectrum" (Fig. 3), though some rocks are clearly borderline cases.

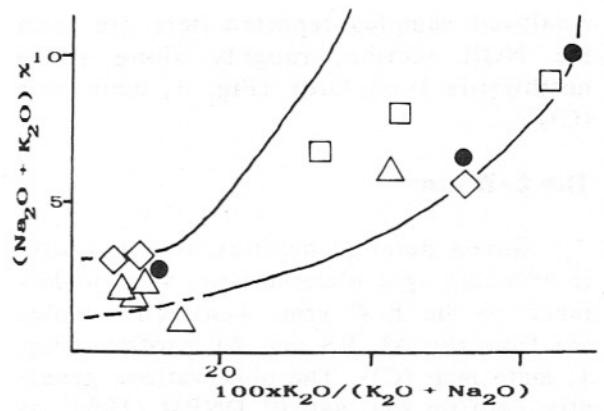


Figure 3 - Hughes' (1973) "igneous spectrum". Symbols as in Figure 2.

The final sample collection includes two clearly ultramafic rocks (AL1, AL3), whose nodular textures may have been formed by deformation of igneous cumulates and subsequent recrystallization. These rocks display post-tectonic blastesis involving radial growth of elongated tremolite-actinolite crystals, which may have been mistaken for spinifex textures by some previous workers (e.g. Mendonça & Braga, 1987).

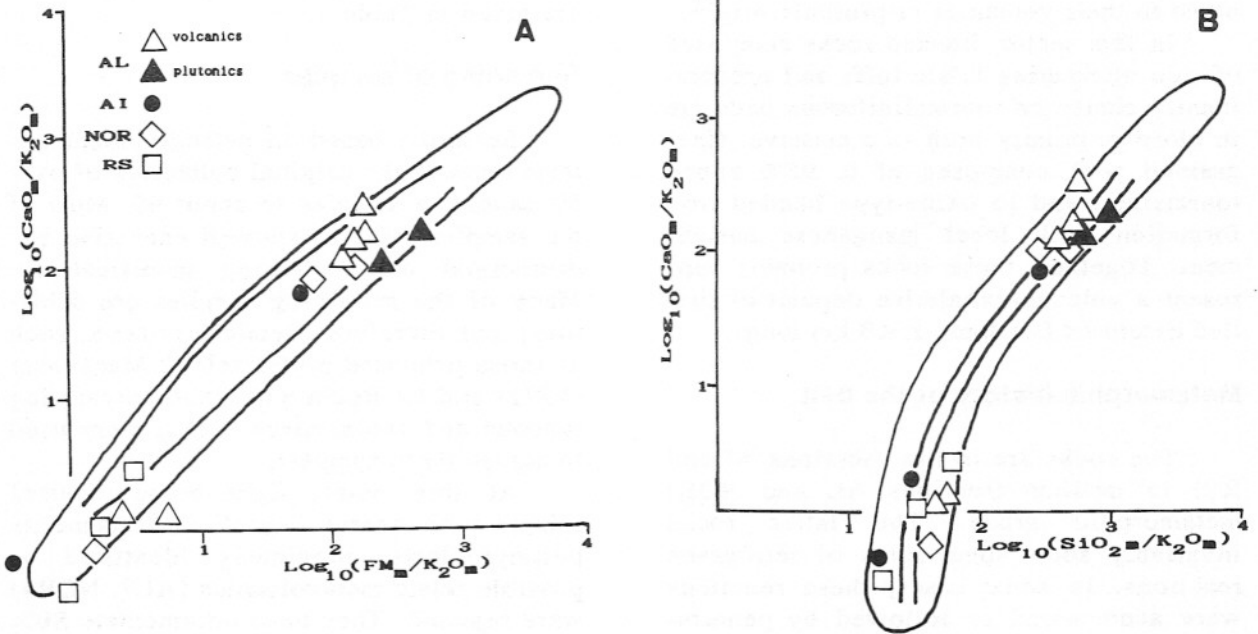


Figure 2 - Selected LMPR plots (A) $\text{FM}/\text{K}_2\text{O}$ vs $\text{CaO}/\text{K}_2\text{O}$ where FM ($\text{FeO}_1 + \text{MgO}$); (B) $\text{SiO}_2/\text{K}_2\text{O}$ vs $\text{CaO}/\text{K}_2\text{O}$ for Orós metavolcanic rocks. Internal bands, igneous trends proposed by Beswick & Soucie (1978); external envelopes include additional analyses (e.g. Gorgona Komatiites: Echeverria (1980); Deception Island (McReath (1975), etc.).

Some of the mafic rocks would not pass the criterion suggested by Pearce (1976) and Condie (1985), $\text{CaO} + \text{MgO} < 20\%$. On the other hand, this criterion would eliminate clinopyroxene or plagioclase-rich, relatively undifferentiated rock types.

Meta-ultramafic rocks

These have the high Ni and Cr contents usually associated with mafic-mineral rich cumulates. Other geochemical characteristics include high TiO_2 (1.8%) and FeO (total) (c. 13%) contents, reflecting the modal abundance of opaque minerals, and also relatively high P_2O_5 (c. 0.37%) content, associated with apatite. High Y contents (c. 60 ppm) are probably associated with the amphibole-rich character of samples, but the relatively high Zr contents are of uncertain origin, since no zircon or baddeleyite grains were identified unequivocally by the conventional optical microscopic examination undertaken.

Metamafic rocks

All examples are subalkaline, with $(\text{Na}_2\text{O} + \text{K}_2\text{O}) < 3.5\%$ at c. 49% SiO_2 (compare with MacDonald & Katsura, 1964; Irvine & Baragar, 1971). K_2O and Rb contents are also low, though these features may be secondary, resulting from K and Rb loss during epidotization or chlorite \pm carbonate formation (e.g. Condie et al., 1977). Mg# values (see e.g. Condie, 1985) show that AL2, AL4, AL5, AL6 and NOR1 are the least differentiated rocks (Mg# = 60-64). Even these are not likely to have been in equilibrium with olivine-bearing mantle (Mg# > c. 70; e.g. Hooper, 1988). Samples AI1 and NOR2 are more differentiated (Mg# = 44 and 40, respectively). Higher Ni and Cr contents are associated with higher Mg# values, suggesting that this common igneous geochemical feature is preserved, but covariance is not well marked, which in turn could point to diverse origins for the different mafic rocks.

Samples from near Aiuába and north of Orós have higher TiO_2 ($2.9 \pm 0.5\%$), P_2O_5 ($0.39 \pm 0.05\%$), Zr (193 ± 43 ppm) and REE (154-204 ppm; sum includes only the elements analysed) than rocks from the Alencar sector, which have $\text{TiO}_2 = 1.07 \pm 0.14\%$, $\text{P}_2\text{O}_5 = 0.11 \pm 0.01\%$, Zr = 71 \pm

16 ppm. REE patterns normalized to Evensen et al. (1978) chondrite values are also different (Fig. 4). The former rocks have LREE-enriched patterns ($\text{Ce}_N/\text{Yb}_N = 4.4-18.9$) with very discrete to significant negative Eu anomalies ($\text{Eu}/\text{Eu}^* = 0.92-0.76$), while the single analysed sample from Alencar has low REE, a rather flat pattern ($\text{Ce}_N/\text{Yb}_N = 2.82$) and no Eu anomaly. A marked La_N deficiency relative to Ce_N and Nd_N is apparent. Although this could be an analytical artefact, since Pr was not determined it is not possible to comment on the possibility that a slight positive Ce anomaly could be present.

The major element tectonic discrimination scheme proposed by Pearce (1976) identifies the unaltered mafic rocks as low-K tholeiites of MORB or CAB/IAT affinities in the Alencar sector, and WPB near Aiuába and north of Orós (Fig. 5). MORB-normalized (Pearce, 1982) spidergrams have some of the geochemical features shown by modern continental WPT (Aiuába, north of Orós) or T-MORB (Alencar), though correspondences are not perfect (Fig. 6).

Metafelsic rocks

These are meta- to slightly peraluminous, subalkaline and have very variable $\text{Na}_2\text{O}/\text{K}_2\text{O}$ ratios. A clear division into two types is possible on the basis of REE patterns (Fig. 7):

(i) concave-up with strong negative Eu anomalies ($\text{Eu}/\text{Eu}^* = 0.48-0.57$) and less extreme LREE/HREE fractionation ($\text{Ce}_N/\text{Yb}_N = 7.3-7.8$) than type (ii). AI2, RS2 and NOR3 are representative of this type, which is thus widely distributed along the belt.

(ii) highly LREE/HREE fractionated ($\text{Ce}_N/\text{Yb}_N = 23.0-49.9$) with an approximately flat to concave-up segment from Dy to Yb, and significant to strong negative Eu anomalies ($\text{Eu}/\text{Eu}^* = 0.42-0.69$). This type occurs in all sectors of the EW arm, but was not found in the NS arm.

Samples of both groups show 2- to 3-fold variations of REE. No relationships between the different REE patterns and $\text{Na}_2\text{O}/\text{K}_2\text{O}$ ratios are found, but some other geochemical differences between the two types occur. Pattern (i) is found in rocks with low K/Rb ratios (83-191), while pattern (ii) occurs in rocks with higher K/Rb ratios (402-1,087) and usually higher

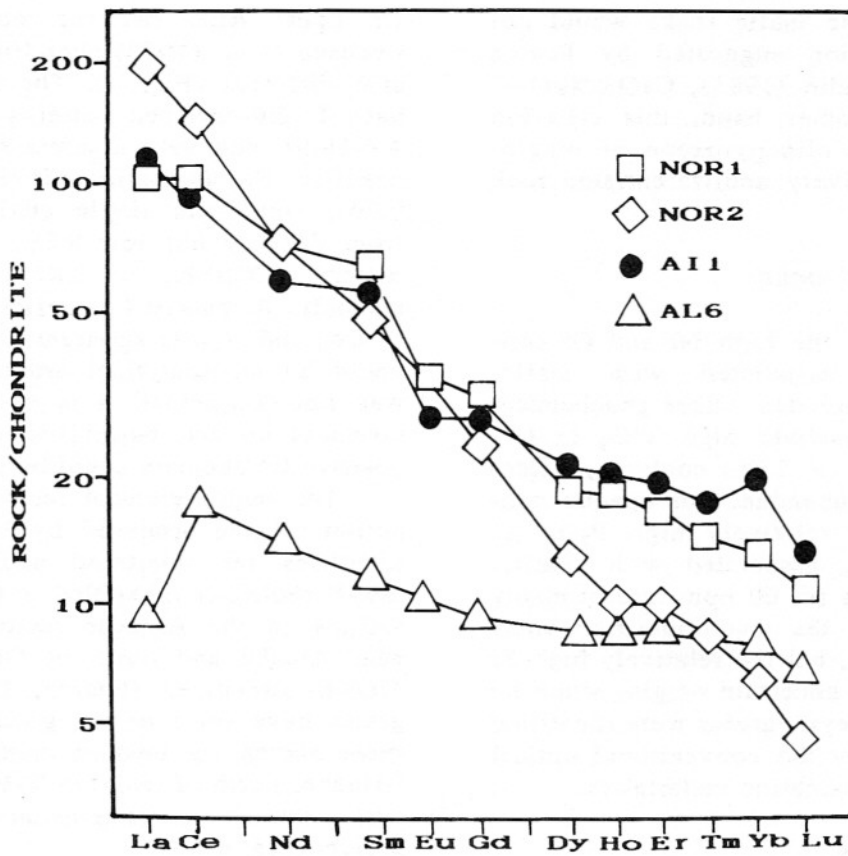


Figure 4 - Rare earth element patterns of mafic meta-volcanic rocks from the Orós belt normalized to Evensen et al. (1978) chondrite values.

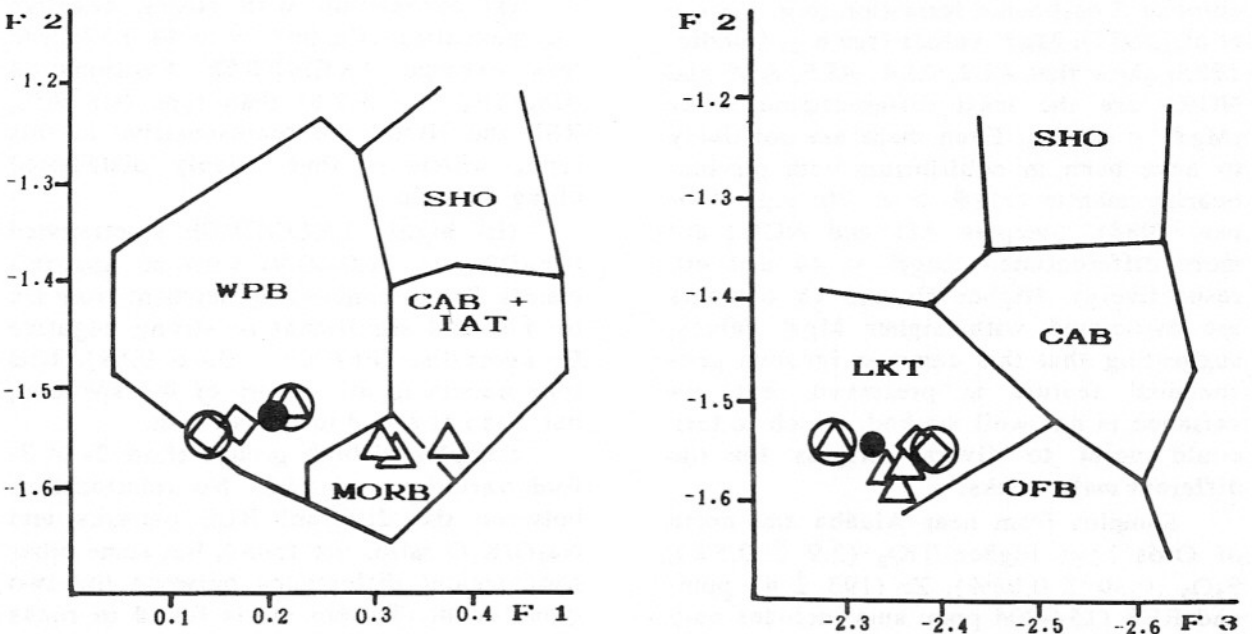


Figure 5 - Pearce (1976) F1-F2 and F2-F3 discrimination diagrams, with fields as originally defined. Symbols as in Figure 2, except those circled, which correspond to modified rocks (see text).

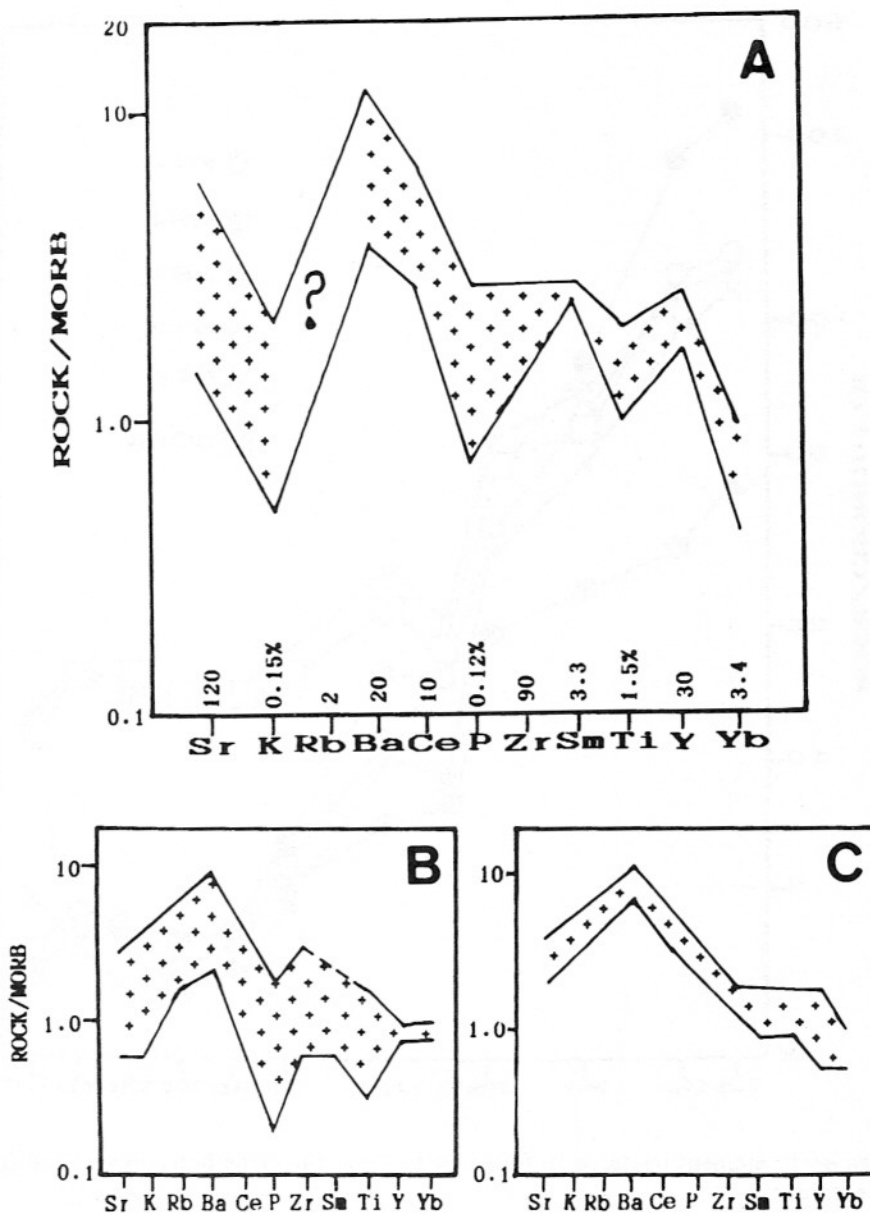


Figure 6 - (A) Envelope of multi-element patterns, normalized to Pearce's (1983) MORB values, for Orós metamafic rocks. (B) Envelope of anomalous patterns for basalts from the northern Atlantic ocean, including Iceland (Wood et al., 1979) and coastal basins of southeastern Brazil (Fodor & Vetter, 1984); (C) Continental WPB according to Pearce (1983).

Ba contents (1,090-1,730 ppm).

ORG-normalized (Pearce et al., 1984) multi-element spectra show steep to very steep inclinations and rather low Sm_N , Y_N and Yb_N values which are typical of some within-plate (WPG) or syn-collision (SCG) granites (Fig. 8).

DISCUSSION AND CONCLUSIONS

The EW arm and part of the NS arm studied here show considerable diversity of volcanic rock types. This diversity is

enhanced by the findings of Sá (1991) and Sá et al. (1991), who describe a mafic-intermediate suite from the NS arm. The mafic rocks are very different from those found in this study, having Mg# in the range 64-48, high K_2O (0.8-2.33%), Rb (23-52 ppm), Sr (398-599 ppm), Ba (346-1,613 ppm) and P_2O_5 (0.4-0.55%), together with low to intermediate TiO_2 (1.2-2.4%) and Zr 160-205 ppm). REE patterns are LREE-enriched ($Ce_N = 105-150$, $Yb_N \sim 18$). Sá (1991) called attention to the great similarity of primitive-mantle-normalized

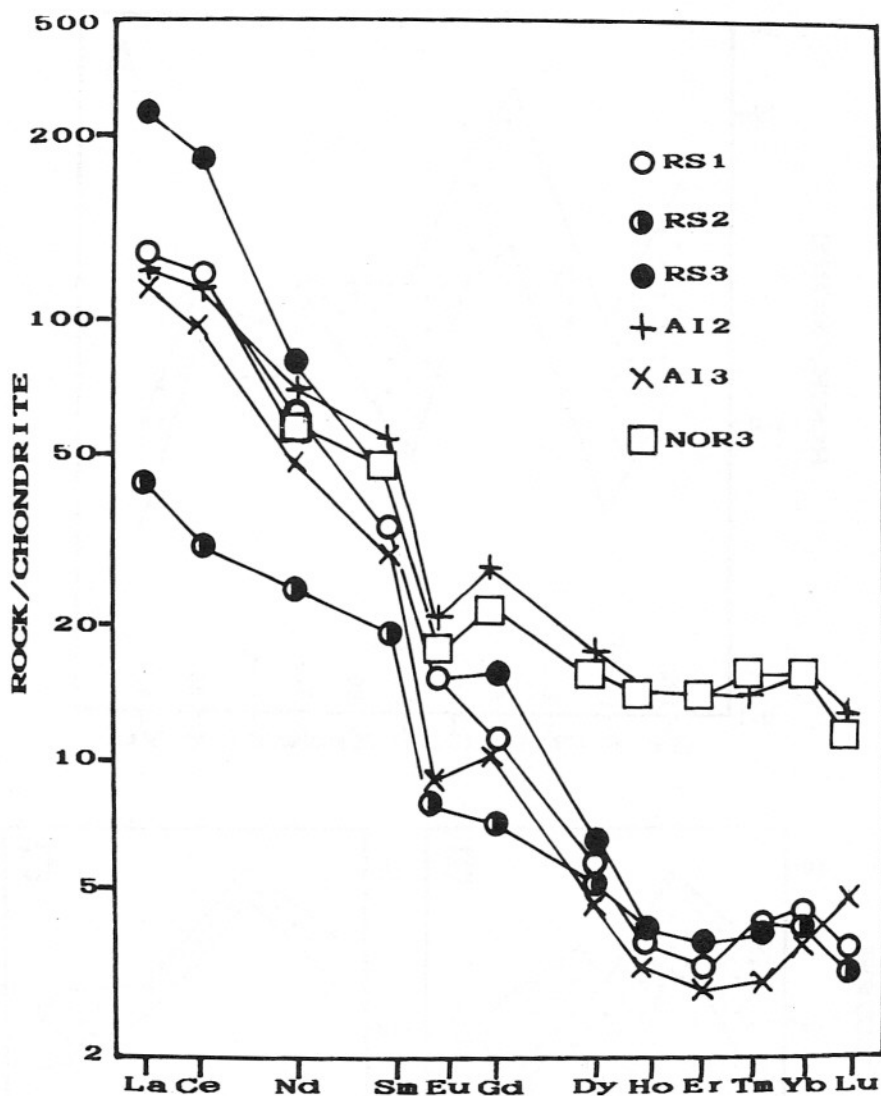


Figure 7 - Rare earth element patterns in felsic rocks from the Orós belt, normalized to Evensen et al. (1978) chondrite values.

“spidergrams” with those of modern volcanic arc shoshonites. A key feature here is the presence of negative Nb anomalies. These are now known to be unspecific as far as tectonic environment is concerned, having also been documented in continental within-plate rocks types (Gibson et al., 1991). The genesis of these anomalies is also not exclusively linked to retention of Nb in refractory phases (e.g. Foley & Wheller, 1990), since they can be generated by equilibration of basaltic magmas with depleted mantle (Keleman et al., 1990).

The “shoshonitic” basalts are associated with andesites which have similar geochemical characteristics. The andesites have Ri values of c. 0.7055, and are

therefore not cogenetic with the more abundant rhyolites of the NS arm, whose Ri values are c. 0.7020. These rhyolites have some of the general geochemical characteristics of the rhyolites found in this study, such as steep, WPG-like spidergrams (Sá, 1991). On the other hand, Sá’s rhyolites have much higher REE (601-644 ppm), K/Rb ratios in the range 170-240, and Ba contents are always high (1,482-2,205 ppm).

Although the diverse rock types are distributed rather unsystematically over a present distance of at least 200 km, all rocks were probably emplaced over a relatively short time span. It is therefore most unlikely that the tectonic environment could have suffered a radical change over

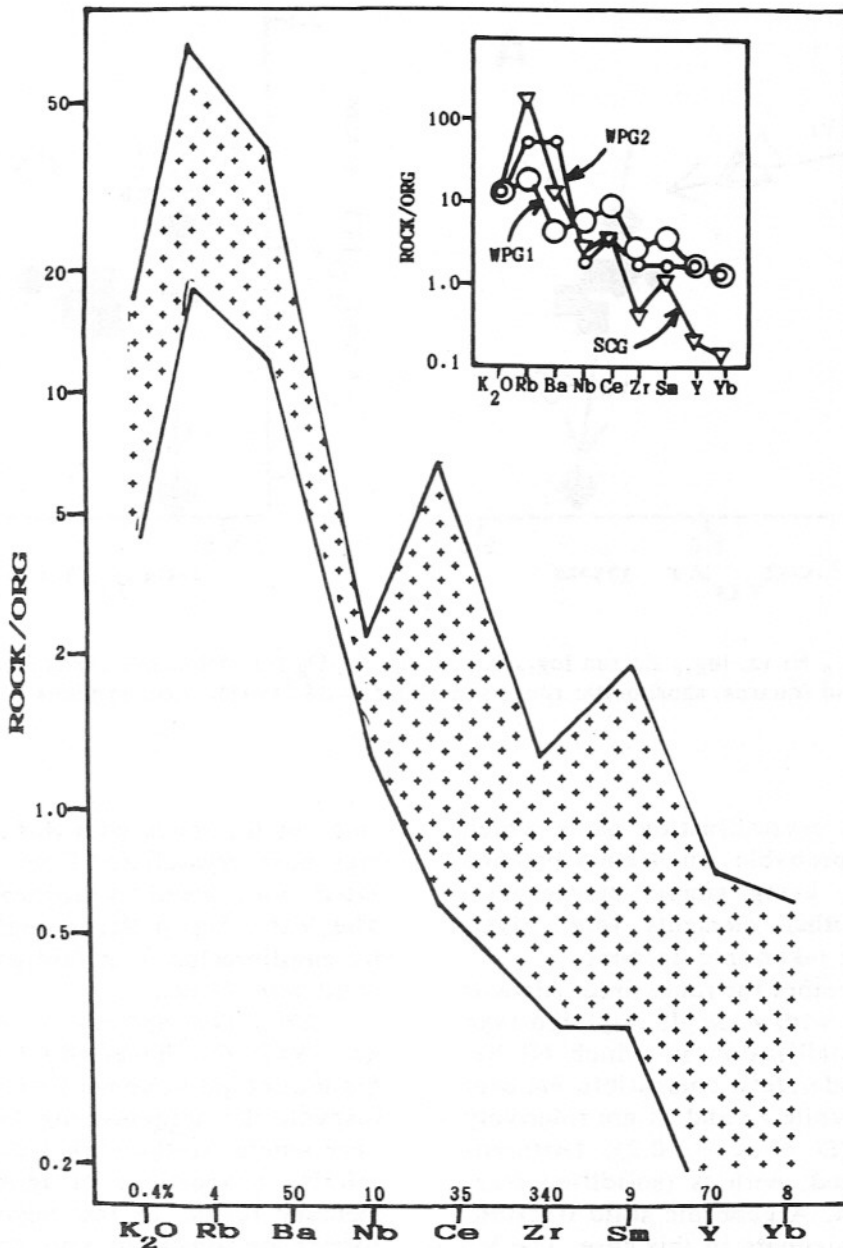


Figure 8 - Envelope of multi-element patterns for felsic metavolcanics, normalized to Pearce et al. (1984) ORG values, with (inset) typical patterns for within-plate (WPG1 & WPG2) and syn-collisional (SCG) types.

this time period, and it is more likely that the diversity of mafic and felsic rocks types is due to heterogeneities in the source rocks, together with different evolutionary histories for the magmas. In some modern cases of the initial phases of continental break-up, mafic rocks may show similar chemical diversity (Fodor & Vetter, 1984). It is outside the scope of this paper to present a detailed analysis of possible petrogenetic schemes for all rock types, especially since the sample popula-

tion of acceptable rocks encountered in this study is small. On the other hand, in the case of the mafic rocks, it is unlikely that the three main types are related to each other by different degrees of melting of similar sources, or by different degrees of fractional crystallization of similar primary magmas. Vector dispositions on trace element diagrams using compatible/incompatible element pairs (e.g. Fig. 9) are very divergent. Vector lengths lead to large differences in degrees of partial melting or

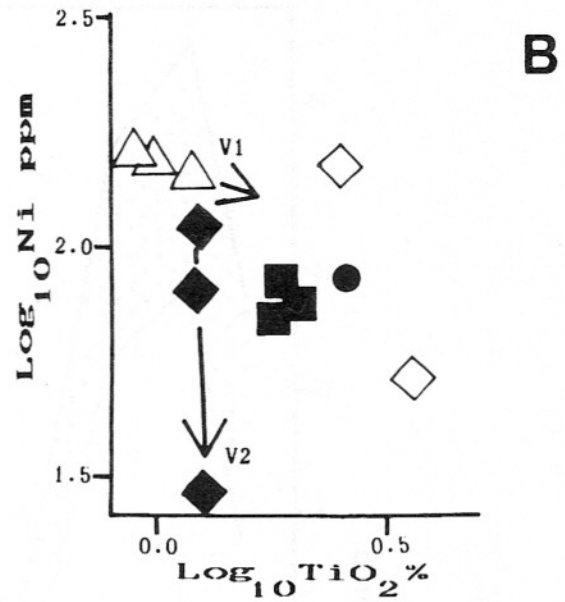
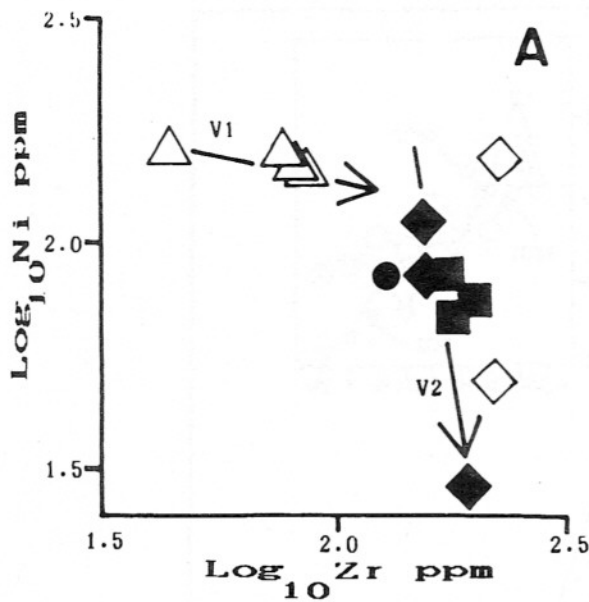


Figure 9 - $\text{Log}_{10} \text{Ni}$ vs. $\text{log}_{10} \text{Zr}$ and $\text{log}_{10} \text{Ni}$ vs. $\text{log}_{10} \text{TiO}_2$ for metamafic rocks from the Orós belt. Full diamonds and squares, shoshonitic rocks according to Sá (1991), other symbols as in Figure 2. See text.

long fractional crystallization paths which are clearly improbable when mass balance considerations, using simple petrogenetic models and other elements (e.g. MgO , P_2O_5 , REE) are taken into account.

The V1 vectors for rocks from Alencar are compatible with a simple Rayleigh-type fractional crystallization in which Ni behaves as a moderately compatible element ($D = c. 1.5$), while Zr and Ti are relatively incompatible ($D = < c. 0.2$). Differentiation is limited, with f_s (solidified fraction) = 0.3-0.4. A gabbroic solid fractionate would be adequate in this case. The V2 vectors for some of the shoshonitic rocks from near Orós require that Ni is more compatible, and Zr and Ti are somewhat less incompatible. These vectors do not explain all chemical variation for the shoshonitic rocks.

In a similar fashion, the felsic rocks have REE patterns which clearly indicate that different mineral/magma equilibria were involved in the genesis of the different types. Published values of mineral/magma distribution coefficients for felsic rocks types (e.g. compilations of Cox, et al., 1979; Henderson, 1984) can be used in a qualitative evaluation.

The steep, hook-shaped patterns are probably generated by amphibole \pm garnet \pm zircon refractory residues or fractionates, while the negative Eu anomalies show that

some of the rocks with this general pattern may have crystallized from magma equilibrated with small quantities of feldspars. The less steep patterns could be produced by equilibration with feldspar \pm amphibole solid assemblages.

Brief descriptions (Mendonça & Braga, 1987; O. Figueiredo Filho & M.C.H. Figueiredo pers. comm.) show that in many respects the neighbouring Jaguaribe belt is very similar to the Orós belt, except in the relative proportions of igneous and sedimentary rocks. In the Jaguaribe belt, the former are somewhat more abundant.

In general, the arenite \pm pelite \pm carbonate sedimentary association indicates rather shallow water conditions, while local occurrences of rhythmites show that some deeper water environments were present. The tourmaliniferous volcano-exhalative deposit requires some continentally-derived input (e.g. Palmer, 1991) and may represent an effusion from a fault associated with graben formation (e.g. Plimer, 1988).

A reasonable tectonic model for the deposition of these two belts envisages initial rifting of slightly attenuated continental crust, accompanied by some escape of basic magmas and a limited quantity of differentiates, derived from very heterogeneous mantle. Much basic magma remained pooled at the base of and within the con-

tinental crust, causing widespread anatexis. Later development of the rift was confined to continued sedimentation, without expressive opening and accompanying formation of an ocean basin.

The Orós belt represents, therefore, a crustal discontinuity formed in the early middle Proterozoic immediately following the c. 2.0 ± 0.2 Ga Transamazonian orogeny. This discontinuity probably played a role during the assemblage of Gondwanaland during the Brasiliano (Pan African). Black & Liégeois (1991) have suggested that, in West Africa, the agglutination of the supercontinent occurred by collage of ancient crustal blocks and younger crustal

components. It is possible that the Orós and Jaguaribe belts correspond to schist belts present in SW Nigeria (e.g. Klemm et al., 1984) and, together with the underlying basement, represent a limit of one of these terranes.

ACKNOWLEDGEMENTS

Thanks are due to Carafba Metais Ind. Com. Ltda for the opportunity to undertake this study, and to J.M. Sá and M.C.H. Figueiredo for useful discussions and commentaries on an early version of the text. Sá is also thanked for permission to cite unpublished data from this thesis.

REFERENCES

- ALMEIDA, F.F.M. de; HASUI, Y.; BRITO NEVES, B.B.; FUCK, R.A. (1981) Brazilian structural provinces: an introduction. *Earth Sci. Rev.*, **17**: 1-29.
- BESWICK, A.E. & SOUCIE, G. (1978) A correction procedure for metasomatism in an Archean greenstone belt. *Precamb. Res.*, **6**: 235-248.
- BLACK, R. & LIÉGEOIS, J.-P. (1991) Pan-African plutonism of the Damagaram inlier, Niger Republic. *Jour. African Earth Sci.*, **13**: 471-482.
- BRAGA, A. de P.F. & MENDONÇA, J.C.G. de S. (1984) Seqüências vulcano-sedimentares de Orós e Jaguaribe - Folha SB24-Z-A-1 - Região Sudeste do Estado do Ceará. In: *Congr. Bras. Geol.*, **33**, Rio de Janeiro, 1984. *Anais*, Rio de Janeiro, SBG, **5**: 2512-2526.
- CONDIE, K.C. (1985) Secular variation in the composition of basalts: an index to mantle evolution. *Jour. Petrol.*, **26**: 545-563.
- CONDIE, K.C.; VILJOEN, M.J.; KABLE, E.J.D. (1977) Effects of alteration on element distributions in Archean tholeiites from the Barberton greenstone belt, South Africa. *Contrib. Mineral. Petrol.*, **64**: 75-89.
- COX, K.G.; BELL, J.D.; PANKHURST, R.J. (1979) *The interpretation of igneous rocks*. Allen & Unwin, London, 450p.
- DNPM (1974) Carta geológica do Brasil ao milionésimo: Folha Jaguaribe (SB24). Departamento Nacional de Produção Mineral, Ministério das Minas e Energia, Brasília.
- DNPM (1983) Mapa geológico do Estado do Ceará. Escala 1:500.000. Departamento Nacional de Produção Mineral, Ministério das Minas e Energia, Brasília.
- DUTRA, C.V. (1984) Método para determinação de traços e sub-traços de terras raras em rochas por espectrometria de plasma (ICP) - aplicação em petrogênese. *Congr. Bras. Geol.*, **33**, Rio de Janeiro, 1984. *Anais*, Rio de Janeiro, SBG, **10**: 4792-3805.
- EVENSEN, N.H.; HAMILTON, P.J.; O'NIONS, R.K. (1978) Rare earth abundances in chondritic meteorites. *Geochim. Cosmochim. Acta*, **42**: 1199-1212.
- ECHEVERRIA, L.M. (1980) Tertiary or Mesozoic komatiites from Gorgona Island, Colombia: field relations and geochemistry. *Contrib. Mineral. Petrol.*, **73**: 253-266.
- FODOR, R.V. & VETTER, S.K. (1984) Rift-zone magmatism: petrology of basaltic rocks transitional from CFB to MORB, Southeastern Brazil margin. *Contrib. Mineral. Petrol.*, **88**: 307-321.
- FOLEY, S.F. & WHELLER, G.E. (1990) Parallels in the origin of the geochemical signatures of island arc volcanics and continental potassic igneous rocks: the role of residual titanates. *Chem. Geol.*, **85**: 1-18.
- GARRELS, R.M. & MACKENZIE, F.T. (1971) *Evolution of sedimentary rocks*. Norton, New York, 396p.
- GIBSON, S.A.; THOMPSON, R.N.; LEAT, P.T.; MORRISON, M.A.; HENDY, G.L.; DICKIN, A.P. (1991) The Flat Tops volcanic field. 1: Miocene open-system, multi-source magmatism at Flander, Trappers Lake. *Jour. Geophys. Res.*, **96**(B6): 13,609-13,627.
- GLADNEY, E.S. & ROELANDTS, I. (1988) 1987 compilation of element concentration data for USGS/BHVO-1, MAG-1, GLO-1, SCo-1, SDC-1, SGR-1 and STM-1. Geos-

- tandards, Newsletter, XII, 253-362.
- GLADNEY, E.S.; JONES, E.A.; NICHOLS, E.J.; ROELANDTS, I. (1990) 1988 compilation elemental concentration data for USGS basalt BCR1. *Geostandards, Newsletter*, XIV, 209-359.
- HENDERSON, P. (1984) General geochemical properties and abundances of the rare earth elements. In: Henderson, P. (Ed.) *Rare Earth Element Geochemistry*, Elsevier, Amsterdam.
- HOOVER, P.R. (1988) The Colombia river basalt. In: MacDougall, J.D. (Ed.) *Continental Flood Basalts*, Kluwer, Dordrecht.
- HUGHES, C.J. (1973) Spilites, keratophyes and the igneous spectrum. *Geol. Mag.*, **109**: 513-527.
- IRVINE, T.N. & BARAGAR, W.R.A. (1971) A guide to the chemical classification of the common volcanic rock. *Can. Jour. Earth Sci.*, **8**: 523-548.
- JOLLY, W.T. (1980) Development and degradation of Archean lavas, Abitibi area, Canada, in the light of major element geochemistry. *Jour. Petrol.*, **21**: 323-363.
- KELEMAN, P.B.; JOHNSON, K.T.M.; KINZLER, R.J.; IRVING, A.J. (1991) High-field-strength element depletions in arc basalts due to mantle-magma interaction. *Nature*, **345**: 521-524.
- KLEMM, D.D.; SCHNEIDER, W.; WAGNER, B. (1984) The precambrian metavolcano-sedimentary sequence east of Ife and Ilesha, SW Nigeria. A Nigerian "greenstone belt"? *Jour. African Earth Sci.*, **2**: 161-176.
- LAFLECHE, M.R.; DUPUYLL, C.; BOUGAULT, H. (1992) Geochemistry and petrogenesis of mafic volcanic rocks of the southern Abitibi belt, Quebec. *Precamb. Res.*, **57**: 207-242.
- LA ROCHE, H. (1972) Résumé sommaire de quelques diagrammes chimico-minéralogiques pour l'étude des associations ignées ou sédimentaires et de leurs dérivés métamorphiques. *Science de la Terre*, **17**: 31-46.
- LECHLER, P.L. & DESILETS, M.O. (1987) A review of the use loss on ignition as a measure of total volatiles in whole-rock analysis. *Chem. Geol.*, **63**: 314-344.
- MACDONALD, G.A. & KATSURA, T. (1964) Chemical composition of Hawaiian lavas. *Jour. Petrol.*, **5**: 82-133.
- MACEDO, M.H. de F.; SÁ, J.M.; KAWASHITA, K. (1988) A idade da faixa Orós: dados preliminares. *Rev. Bras. Geoc.*, **18**: 362-368.
- MENDONÇA, J.C.G. de S. & BRAGA, A. de P.G. (1987) As faixas vulcano-sedimentares de Orós e Jaguaribe: um "greenstone belt"? *Rev. Bras. Geoc.*, **17**: 225-241.
- McREATH, I. (1975) Geochemistry of Deception Island. In: Baker, P.E.; McReath, I.; Harvey, M.R.; Roobol, M.J.; Davies, T.G. *The Geology of the South Shetland Islands*. V. Volcanic evolution of Deception Island. British Antarctic Survey Scientific Report 78.
- PALMER, M.R. (1991) Boron isotope systematics of hydrothermal fluids and tourmalines: a synthesis. *Chem. Geol. (Isotope Geochemistry Section)*, **94**: 111-122.
- PEARCE, J.A. (1976) Statistical analysis of major element patterns in basalt. *Jour. Petrol.*, **17**: 15-43.
- PEARCE, J.A. (1982) Trace element characteristics of lavas from destructive plate boundaries. In: R.S. Thorpe (Ed.) *Andesites*, Wiley, New York.
- PEARCE, J.A.; HARRIS, N.B.W.; TINDLE, A.G. (1984) Trace element discrimination diagrams for the tectonic interpretation of granitic rocks. *Jour. Petrol.*, **25**: 956-983.
- PLIMER, I.R. (1988) Tourmalinites associated with Australian proterozoic submarine exhalative ores. In: G.H. Friedrich & P.M. Herzig (Eds.) *Base Metal Sulfide Deposits*, Springer Verlag, Berlin.
- RIES, A.C. (1977) Stromatolites in the Ceará group (precambrian) in Brazil. *Simp. Geol. Nordeste, VII, Campina Grande, Anais, Campina Grande, SBG*, **1**: 366-391.
- SÁ, J.M. (1991) Évolution géodynamique de la ceinture proterozoïque d'Óros, nord-est du Brésil. Thèse de Docteur, Université de Nancy I, France, 177p.
- SÁ, J.M.; BEZERRA, F.H.R.; MACEDO, M.H.F.; PEREIRA, R. (1988) Middle proterozoic supracrustals and Brasiliano orogeny in the southeast Ceará state: a monocyclic evolution. *Congr. Lat. Amer. Geol.*, **7**, Belém, Brazil, Anais, Belém, SBG, **1**: 35-48.
- SÁ, J.M.; BERTRAND, J.M.; LETERRIER, J. (1991) Evolution géodynamique et géochronologie (U-Pb, Rb-Sr et K-Ar) de la ceinture plissée d'Óros, NE du Brésil. *Comptes Rendus Acad. Sci., Paris*, t. 313, Sér. II, 231-237.
- SANTOS, E.J. dos & BRITO NEVES, B.B. de (1984) Província Borborema. In: Almeida, F.F.M. de & Hasui, Y. (coordinators) *O Pré-Cambriano do Brasil*, Edgard Blücher, São Paulo.
- SANTOS, E.J. dos; COUTINHO, M.G. de N.; COSTA, M.P. de A.; RAMALHO, R. (1984) A região de dobramentos nordeste e a bacia de Parnaíba incluindo o cráton de São Luis e as bacias marginais. In: Schobbenhaus, C.; Campos, D. de A.; Dreze, G.H.; Asmus, H.E. (Eds.) *Geologia do Brasil*, Departamento Nacional de Produção Mineral/Companhia de Pesquisas de Recursos Minerais, Brasília.
- WOOD, D.A.; JORON, J.L.; FRENILLE, M.; NORRY, M.; TARNEY, J. (1979) Elemental and Sr isotope variations in basic lavas from Iceland and the surrounding ocean floor. The nature of mantle source inhomogeneities. *Contrib. Mineral. Petrol.*, **70**: 319-340.

APPENDIX - Brief sample descriptions

Section AI

AI1 - Fine-grained chloritic schist with minor late epidote and oxidation.

AI2 - Felsic schist with minor chlorite.

AI3 - Mylonite with quartz porphyroclasts and white mica.

Section RS

RS1 - Felsic schist with microcline porphyroclasts, biotite, little late-stage transformation (meta-tuff)?

RS2 - Felsic schist with microcline porphyroclasts and some late white mica.

RS3 - Felsic schist with late chlorite and white mica.

Section AL

AL1 - Medium-grained nodular meta-ultramafic rock with schistose matrix. Early hornblende overgrown by chlorite \pm tremolite-actinolite, but no other late products.

AL2 - Fine to medium-grained amphibole schist with mosaic aggregates of small plagioclase crystals, possibly former phenocrysts. Rather abundant late epidote \pm chlorite + carbonate minerals.

AL3 - Massive nodular fine to medium-grained amphibolite with hornblende reacting to actinolite and late epidote + chlorite + carbonate minerals.

AL4 - Amphibolite with possible relict plagioclase phenocrysts, little actinolite and almost no later products.

AL5 - Fine to medium-grained amphibolite, little actinolite and no late products.

AL6 - Somewhat nodular amphibolite with schistose matrix, little actinolite and no late products.

AL7 - Fine to medium-grained biotite schist.

AL8 - Pyritiferous banded cherty felsic tuff.

AL9 - Felsic schists with quartz eyes and magnetite porphyroblasts.

Section NOR

NOR1 - Fine to medium-grained actinolite schists with possible relict plagioclase phenocrysts, early epidote and some late products.

NOR2 - Plagioclase-phyric, strongly epidotized and actinolitized meta-basalt with minor late epidote.

NOR3 - Mylonitic meta-quartz porphyry.

NOR4 - Felsic schist with quartz eyes and magnetite porphyroblasts.